Video Article

# Analysis of $^{18}$FDG PET/CT Imaging as a Tool for Studying *Mycobacterium tuberculosis* Infection and Treatment in Non-human Primates

Alexander G. White*[1], Pauline Maiello*[1], M. Teresa Coleman[1], Jaime A. Tomko[1], L. James Frye[1], Charles A. Scanga[1], Philana Ling Lin[2], JoAnne L. Flynn[1]

[1]Department of Microbiology and Molecular Genetics, University of Pittsburgh School of Medicine

[2]Department of Pediatrics, Children's Hospital of Pittsburgh, University of Pittsburgh Medical Center

*These authors contributed equally

Correspondence to: JoAnne L. Flynn at joanne@pitt.edu

URL: https://www.jove.com/video/56375
DOI: doi:10.3791/56375

Keywords: Infection, Issue 127, PET/CT Imaging, *Mycobacterium tuberculosis*, region-of-interest analysis, non-human primates, FDG, granulomas, lymph nodes, inflammation

Date Published: 9/5/2017

Citation: White, A.G., Maiello, P., Coleman, M.T., Tomko, J.A., Frye, L.J., Scanga, C.A., Lin, P.L., Flynn, J.L. Analysis of $^{18}$FDG PET/CT Imaging as a Tool for Studying *Mycobacterium tuberculosis* Infection and Treatment in Non-human Primates. *J. Vis. Exp.* (127), e56375, doi:10.3791/56375 (2017).

## Abstract

*Mycobacterium tuberculosis* remains the number one infectious agent in the world today. With the emergence of antibiotic resistant strains, new clinically relevant methods are needed that evaluate the disease process and screen for potential antibiotic and vaccine treatments. Positron Emission Tomography/Computed Tomography (PET/CT) has been established as a valuable tool for studying a number of afflictions such as cancer, Alzheimer's disease, and inflammation/infection. Outlined here are a number of strategies that have been employed to evaluate PET/CT images in cynomolgus macaques that are infected intrabronchially with low doses of *M. tuberculosis*. Through evaluation of lesion size on CT and uptake of $^{18}$F-fluorodeoxyglucose (FDG) in lesions and lymph nodes in PET images, these described methods show that PET/CT imaging can predict future development of active versus latent disease and the propensity for reactivation from a latent state of infection. Additionally, by analyzing the overall level of lung inflammation, these methods determine antibiotic efficacy of drugs against *M. tuberculosis* in the most clinically relevant existing animal model. These image analysis methods are some of the most powerful tools in the arsenal against this disease as not only can they evaluate a number of characteristics of infection and drug treatment, but they are also directly translatable to a clinical setting for use in human studies.

## Video Link

The video component of this article can be found at https://www.jove.com/video/56375/

## Introduction

*Mycobacterium tuberculosis* has plagued humans for millennia and causes more mortality than any other single infectious agent in the world today. In 2015, there were 10.5 million reported new cases of tuberculosis (TB) globally[1] with the majority of cases emanating from India, Indonesia, China, Nigeria, Pakistan, and South Africa. Estimates place the global death toll from TB at 1.4 million people during that same time period. This value is nearly 25% lower than the death rate 100 years ago. Although drug sensitive TB is treatable, the regimen is lengthy requiring multiple medications and compliance is a concern. The emergence of multi drug-resistant (MDR) strains accounted for ~580,000 of the new TB cases in 2015. The successful treatment rate of patients with MDR strains of *M. tuberculosis* is only estimated to be around 50%. Even more alarming is the emergence of extensively resistant (XDR) strains of *M. tuberculosis*, which are resistant to nearly every available drug. Thus, new techniques are needed within the TB research field that enhance the ability to diagnose TB, increase the immunological understanding of the disease process, and allow for the screening of novel treatments and prevention strategies including antibiotic regimens and vaccine efficacy studies.

*M. tuberculosis* is an aerobic acid-fast bacillus that is physically characterized by its very complex outer cell wall and slow growth kinetics. Infection generally occurs through inhalation of individual bacteria contained in aerosolized droplets that are expelled from a symptomatic, infected individual while coughing, sneezing, or singing. Of the exposed individuals that develop infection, only 5 - 10% of people develop active clinical TB. The remaining 90% have a varying spectrum of asymptomatic infections that ranges from subclinical infection to no disease at all, all of which is classified clinically as latent TB infection (LTBI)[2,3]. Of the population that has this asymptomatic infection, approximately 10% will develop active TB by reactivation of the contained infection in their lifetime. The risk of reactivation dramatically increases if a person with asymptomatic infection contracts HIV or undergoes treatment with an immunosuppressive drug, such as TNF inhibitors[4,5,6]. Active TB disease also presents as a spectrum, with most people having pulmonary TB, which affects the lungs and thoracic lymph nodes. However, *M. tuberculosis* can infect any organ, so that the infection can also present in extrapulmonary sites of involvement.

 

The pathologic hallmark of *M. tuberculosis* infection is an organized spherical structure of host cells, called the granuloma. Macrophages, T cells and B cells are major components of the granuloma, with variable numbers of neutrophils[7]. The center of the granuloma is often necrotic. Thus, granulomas function as an immune microenvironment to kill or contain the bacilli, preventing spread to other parts of the lungs. However, *M. tuberculosis* can subvert killing by the granuloma, and persist within these structures for decades. Consistent and regular monitoring for the development of active TB disease after new infection or reactivation of LTBI is impractical, scientifically challenging and time consuming. Techniques that study these processes longitudinally, in humans and human-like animal models, are extremely useful to the scientific community in furthering the understanding of the many complexities of *M. tuberculosis* infection and disease.

PET/CT is an extremely useful imaging technique that has been employed to study a vast range of disease states in humans and animal models[8]. PET is a functional technique that uses positron-emitting radioactive compounds as a reporter. These radioisotopes are typically functionalized to a metabolic compound, such as glucose, or to a targeting group that is designed to bind to a receptor of interest. Since the radiation emitted from PET isotopes is powerful enough to penetrate tissue, very low concentrations can be used which allows for study below saturation levels in receptor-targeting compounds and at a low enough concentration to have no impact on metabolic processes when using agents such as 2-deoxy-2-($^{18}$F)Fluoro-D-glucose (FDG). CT is a three-dimensional x-ray imaging technique that uses varying levels of x-ray attenuation to identify physical characteristics of organs within the body[9]. When paired with PET, CT is used as a map to determine specific locations and structures that show uptake of a PET radiotracer. PET/CT is a powerful tool for *in vivo* imaging of both humans and animal models infected with *M. tuberculosis* infection that has led to many important insights into pathogenesis, response to drug treatment, disease spectrum, etc[6,10,11,12]. This work describes specific PET/CT analytical methods to study TB in non-human primate models longitudinally using parameters such as granuloma size, FDG uptake in individual lesions, whole lung and lymph node FDG avidity, and detection of extrapulmonary disease[6,10,11,12].

This manuscript describes methodologies of imaging analysis in non-human primates (NHPs), specifically cynomolgus macaques, which are used to longitudinally evaluate disease progression and drug treatment following infection with *M. tuberculosis*. NHPs are a valuable animal model because when inoculated with a low dose of *M. tuberculosis* Erdman strain, animals show a variety of disease outcomes with ~50% developing active TB and the remaining animals having asymptomatic infection (*i.e.* controlling the infection, LTBI), providing the closest model to the clinical disease spectrum seen in humans[3,13,14,15,16]. Reactivation of LTBI in macaques is triggered by the same agents that cause reactivation in humans, examples of which include human immunodeficiency virus (HIV, using simian immunodeficiency virus (SIV) as the macaque version of HIV), CD4 depletion or tumor necrosis factor (TNF) neutralization[13,16]. In addition, macaques present with pathology that is extremely similar to that seen in humans, including the organized granulomas that form in lungs or other organs[17]. Thus, this model has provided important insights into the basic host-pathogen interactions in *M. tuberculosis* infection, as well as valuable knowledge about drug regimens and vaccines for tuberculosis[14,18,19,20,21].

PET/CT imaging provides the ability to follow the appearance, distribution, and progression of individual granulomas. This work has primarily used FDG as a probe, which, as a glucose analogue, incorporates into metabolically active host cells, such as macrophages, neutrophils, and lymphocytes[8], all of which are in granulomas. Thus, FDG is a proxy for host inflammation. The analysis procedures detailed herein uses OsiriX, a widely used DICOM viewer available for purchase and use. The image analysis methods described track the shape, size, and metabolic activity (*via* FDG uptake) of individual granulomas over time and uses imaging as a map for identifying specific lesions upon animal necropsy. Additionally, a separate method has been developed that quantifies the summation of FDG uptake in the lung above a specific threshold (SUV ≥ 2.3) and uses this value to evaluate differences between control and experimental groups across studies ranging from vaccine trials to co-infection models. These data support that this overall measure of FDG uptake in lungs is correlated with bacterial burden, thus providing information about the disease status. Similar analyses can be performed on the FDG uptake of thoracic lymph nodes to study progression of disease as well. The following protocol describes the experimental process from animal infection through image analysis.

## Protocol

All methods outlined in this work have been approved by the University of Pittsburgh Institutional Animal Care and Use Committee. All procedures followed institutional biosafety and radiation safety requirements. CT scanning requires donning lead apron and throat cover. Biosafety Level 3 (BSL3) garb and procedures for working with non-human primates must be followed according to institutional guidelines. All scanning was performed in a BSL3 facility.

# 1. Animal Infection Procedure

1. Sedate animal with ketamine (10 mg/kg, intramuscular) or telazol (5 - 8 mg/kg, intramuscular) if animal has adverse reactions to ketamine.
2. Using a laryngoscope, visualize the epiglottis and vocal cords. Anesthetize vocal cords by spraying with cetacaine spray for ~ 1 s (no more than 2 s).
3. Using the laryngoscope, guide a bronchoscope (2.5 mm outer diameter) into the trachea *via* direct visualization into the right caudal lung lobe.
4. Prepare a syringe consisting of approximately 5 - 20 (depending on study) colony forming units of *M. tuberculosis* in 2 mL of sterile saline and administer the solution through the bronchoscope channel. Prepare a separate syringe consisting of 2 mL sterile saline and administer the saline through the bronchoscope channel followed by 5 mL air to ensure complete deposition of bacteria[22].
5. Withdraw the bronchoscope and observe the monkey until fully awake and alert.

# 2. Imaging Acquisition, Histogram, and Reconstruction Procedure

1. Prepare animal for imaging.
    1. Sedate animal with ketamine (10 mg/kg, intramuscular) or telazol (5 - 8 mg/kg, intramuscular) if animal has adverse reactions to ketamine.

NOTE: Animals need to be fasted overnight to reduce risk of vomiting during the imaging procedure and to maintain consistency in FDG PET scans.
2. Insert an intravenous (IV) catheter into the saphenous vein of either leg and secure with cloth tape.
3. Dilute an approximately 5 millicurie dose of FDG with sterile saline to a total volume of 5 mL in a plastic syringe.
4. Record the pre-injection radioactivity level in the syringe using a dose calibrator, record the time, and place the syringe in a lead syringe holder.
5. Slowly inject the radioactive dose through the IV catheter and follow with 5 mL of sterile saline. Record the injection time. Injection time should be coordinated to be approximately 45 min - 1 h before PET imaging.
6. Record the post-injection radioactivity level of the syringe using the dose calibrator and record the time. Dispose of the syringe in an appropriate waste container.
7. Using a laryngoscope, visualize the epiglottis and vocal cords and anesthetize with cetacaine spray.
8. Guide an endotracheal tube (3.5 mm - 4.5 mm depending on monkey size) into the trachea and inflate the cuff at the inserted end of the tube.
9. Using a long thin strip of sterile gauze, secure the intubation tube by wrapping the strip around the tube, piercing the strip with each canine of the animal, then tie a knot with the remaining amount of gauze around the bridge of the snout and finally around the back of the head.
10. Cover the eyes with artificial tears to prevent drying out during imaging.

2. Perform CT and PET scans.
    1. Place animal on scanning bed.
    2. Connect intubation tube to a respirator with the following settings: Respiration rate = 15, Peak Pressure = 15 - 17, Oxygen% = 40, PEEP (positive end expiratory pressure) = 3, Tidal Volume = 60, $T_i$ (Inspiratory time) = 0.4, I:E (inspiratory to expiratory time) Ratio = 1:3.4, $T_{plateau}$ (inspiratory pause before expiration)= 0.5, Peak Flow = 9.0 (these values can be adjusted based on the animal specific pulmonary compliance or experimental needs).
    3. Start inhalant anesthesia (2% isoflurane) through the ventilator and continue until animal shows no reaction to physical stimuli.
    4. Place animal in a prone position with head and legs supported.
    5. Place animal within the CT field-of-view and conduct a preview scan to ensure that the entire span of lung volume will be included in the full scan.
    6. Acquire a CT scan with the following parameters (Helical scan, Axial FOV = 250 mm, Voltage = 140 kV, Current = 2.0 mA, Slice Thickness = 1.25 mm, Sharpness = extra sharp) while conducting a ventilator breath hold.
    NOTE: Contrast agent CT is optional. If performing a contrast scan, a delay is necessary between injection of contrast agent and image acquisition because pooling of contrast agent in the heart interferes with proper image reconstruction of the lung space on the PET scan and creates artifact in the lungs on the CT scan
    7. Be sure to lower isoflurane concentration to 0.7 - 0.8% during the scan procedure.
    8. Place animal within the PET field-of-view.
    NOTE: The system in place for this work is an inline system with a separate CT and PET scanner. Coordinates for PET positioning are manually calculated based on CT coordinates.
    9. Acquire 600 s PET images for each bed position.
    NOTE: The Focus 220 system has an axial FOV of 7.6 cm. This work was performed using four bed positions that are manually stitched during post-processing.
    10. Turn isoflurane off, wean animal off ventilator gradually, remove air from the ventilator tube cuff and remove the tube once the animal has regained coughing reflexes and is breathing normally. Remove IV catheter and hold pressure on the injection site until blood flow has stopped.

3. Perform PET image histogram and reconstruction.
    1. Perform PET image histogram with the following parameters: 3D histogram with no smoothing, span: 3, ring difference: 47, global average deadtime correction.
    2. Perform PET image reconstruction with the following parameters = OSEM3D (Ordered Subset Expectation Maximum-3 Dimension) algorithm with CT-based attenuation, ramp projection filter, and scatter correction yielding a 284-slice image.

4. Co-register PET and CT images.
5. Export Co-registered PET and CT DICOM images to the software (*e.g.*, OsiriX).

## 3. Identifying and Analyzing Individual Lesions

1. Open PET and CT DICOM images from the OsiriX database in the axial orientation (CT image will be fused with the PET image and there will be a separate PET image window).
2. Set scan (or serial scans) to axial orientation.
3. Click (anywhere) on the CT scan and change the **"WL/WW"** in the top menu bar to **"CT – Pulmonary "**.
4. Scroll through the scan to determine where lung lobes begin and end. (Identify lung fissures.)
    1. Scroll through the entire scan, focusing on small areas of lung space at a time.
    2. Notice that normal lung appears dark and anatomical features appear lighter (depending on density). Airways appear black while vasculature appears nearly white.
    3. Follow vessels and airways as they appear to move while scrolling through axial slices.
    4. Fissures can be identified in areas where there are no vessels or airways. (These are areas in the lung that appear only dark with no other anatomical structures.)

5. Use the fused PET/CT to identify lesions.
    1. Scroll through the entire scan, focusing on small areas of lung space at a time.
    NOTE: Focus on one lung lobe at a time to identify and count lesions.

2. Identify FDG-avid lesions within the lung. They will look like hot spheres - very different from lung background. Small, cold lesions will be much less obvious and harder to identify. They will appear on scan as dense structures that do not move while scrolling (as vessels do).
   NOTE: Small lesions and vessels look very similar. An easy way to distinguish between the two is to hover the cursor over the structure in question and scroll up and down a slice or two. If the structure stays underneath the cursor, the structure is a lesion. If the structure moves away from the cursor while scrolling up or down a slice, it is most likely vessel or airway.
3. For identification purposes, use the **"Arrow"** tool to point to each lesion on the scan.
4. For location purposes, use the **"Point"** tool and click on the lesion so that the ROI (region of interest) is directly in the center of the granuloma. Information contained in this ROI will include the Cartesian coordinates (XYZ-coordinates) where the lesion can be found.

6. Use the "Length" and "Oval" tools to measure size (mm) and FDG avidity (SUV) of each lesion.
   1. To measure size of a lesion, remove the PET signal so that only the CT is visible.
   2. Choose the **"Length"** tool.
   3. Scroll until the slice that contains the largest portion of the lesion is identified (the slice where the lesion appears to be largest).
   4. Draw a line across the longest length of the lesion. The info included in this ROI will represent the length (in mm) of the diameter of the lesion.
   5. To measure the FDG avidity of a lesion, first click on the PET scan and turn up the PET. Go to the **"WL/WW & CLUT"** Osirix menu on the top of the screen and choose **"Set WL/WW Manually"** in the WL/WW dropdown menu. In the dialogue box, enter *0* into the **"From"** and *20* into **"To"** in order to limit the window from 0 to 20 SUV.
   6. Choose the **"Oval"** tool from the **"Mouse button function"** tool dropdown menu.
   7. Scroll over the lesion to assess the hottest portion of the lesion. Draw an oval around the lesion. The **"Oval"** tool ROI information includes descriptive statistics for all SUVs in voxels within the region. Record the *maximum SUV* within the region.
   8. As each **"Oval"** ROI only represents the SUV values for that specific axial plane of the lesion and typical lesions are spherical in shape, draw ovals on several slices to ensure that the actual maximum SUV of the lesion is captured.
      NOTE: If the PET/CT scans are manually reconstructed, the PET and CT images might not be perfectly matched. If this is the case, all SUV analyses and ROIs should be conducted on the PET scan instead of the fused PET/CT scan. Because many lesions are smaller than the resolution of the PET detector crystals, all measured SUVs for individual lesions are entered into a recovery coefficient calculator spreadsheet that performs a partial volume correction for each lesion[23].

## 4. Total Lung FDG Avidity Measurement Procedure to Determine Total Lung Inflammation

1. Open PET and CT DICOM images from the OsiriX database in the axial orientation (CT image will be fused with the PET image and there will be a separate PET image window).
2. Perform a segmentation of the lung volume on the CT image.
   1. Click anywhere on the CT scan to make sure it is the active window.
   2. Go to **ROI** dropdown menu and select **"Grow Region (2D/3D) Segmentation…"**.
   3. In order to capture the density of normal lung, set the Lower Threshold to -1024 and the Upper Threshold to -200. These are indicative of Hounsfield Units, though the segmentation box does not name them as such.
   4. Once the lower and upper thresholds are set, click anywhere inside the lung. The entire lung should appear highlighted in green.
   5. Next, click on **"Compute"** in the Segmentation Parameters dialog box. This will expand the grow region from one slice to the entire lung volume.

3. Move the "grow region" of the lungs from the CT scan to the PET scan.
   1. Click on the small icon to the left of the name of the CT scan and drag the icon to the PET scan.
   2. Select **"Copy ROIs"**. There should now be an overlay of the lungs on the PET scan.

4. Delete ROI from CT scan (optional).
   NOTE: It helps to be able to see the entire lung without ROIs on the CT scan to make sure that all pathology in the lung is captured. To do this, delete the ROIs. Make sure the CT window is active (click on the CT scan) select the **ROI** dropdown menu and select **"Delete All ROIs in this Series."**
5. Fill in high-density areas of the lung that appear as gaps on the PET scan.
   NOTE: On many occasions, there are holes in the ROI on the PET scan where the lung tissue was denser than -200 HU on the CT scan (this step can be skipped if it does not occur).
   1. Highlight the **ROI** dropdown menu and select **"Brush ROIs"** → **"Closing."** When the dialog box appears, slide the arrow to 3 so that the top of the dialog box reads **"Structuring Element Radius: 3"** and check **"Apply to all ROIs with the same name."**
      NOTE: When there are large portions of disease (such as consolidations which are denser than surrounding lung tissue), often closing the brush ROIs will not be sufficient to fill in the entire lung. If this is the case, the gaps must be filled in manually.
   2. Go to the "Mouse button function" area on the top menu and click on the small arrow on the right.
   3. Select the **"Brush"** tool.
   4. Once this tool is selected, manually draw within the ROI to fill in the holes.

6. Isolate lung ROI on PET scan.
   1. Now that there is a representation of the entire lung on the PET scan, delete all pixels outside the lung.
   2. Highlight the **ROI** dropdown menu and select **"Set Pixel Values to…"**.
   3. Click the **Outside ROI** check box and set all pixels outside the ROI to 0.

7. Isolate "hot" pathology.
   1. Use any threshold that is desired to be used as "hot." SUVs greater than 2.3 are considered to be "hot" based on literature values for tuberculosis lesions[24].

2. Select the **ROI** dropdown menu and select **"Set Pixel Values to…"**.
3. Click the **Inside ROI** check box. Make sure to click the "and" box so that all values between 0 **and** 2.3 are set to 0.

8. Make sure only disease pathology is accounted for in the ROI.
    1. Note that there are areas (such as the liver) that are hotter than 2.3. Ensure that only desired areas are captured by deleting the ROIs and creating another grow region. Other common tissues that interfere at this time include the heart, mediastinal lymph nodes, vertebrae, and ribs.
    2. Highlight the **ROI** dropdown menu and select **"Delete All ROIs in this Series."** Next, go to **ROI** and select **"Grow Region (2D/3D) Segmentation…"**.
    3. Change the threshold to Lower Threshold to 2.3 and the Upper Threshold to 100.
    4. Scroll through the entire PET window, clicking on disease pathology and clicking **"Compute."** Repeat for every area of hot disease. Be sure to save whole lung ROI by using the **"Save ROIs"** option under the ROI menu.

9. Export raw values into a spreadsheet.
    1. Go to **2D Viewer** in the dropdown menu bar and select **"Revert Series."**
    2. Next, go to the **Plugins** dropdown menu bar.
    3. Select **"ROI Tools"** → **" Export ROIs."** Name and save the exported raw data file. Be sure to select **"CSV"** at the bottom of this dialog box.

10. Calculate the Total FDG Avidity from the raw data. Each row in this spreadsheet represents a single slice from the scan. The column of interest is **"RoiTotal."**
    1. In order to calculate the "Total FDG avidity," add all of the **"RoiTotal"** of the slices together. Calculate the sum of Column F (RoiTotal). This sum is the Total FDG avidity measurement.
    2. If OsiriX does not have the Export ROI plug-in, go to **Plugins** in the dropdown menu. Select **"Plugins Manager…"** Click on the **"Download…"** Tab at the top of the dialog box. Select **"ExportROIs"** from the **"Available plugins"** dropdown menu. Select **"Download & Install."**

## 5. Analytical Procedure to Determine FDG Uptake in "Hot" Lymph Nodes

1. Open PET and CT DICOM images from OsiriX database in the axial orientation (CT image will be fused with the PET image and there will be a separate PET image window).
2. Ensure that while performing manual ROI analysis on PET images that the image intensity window be consistent.
    1. Click on the PET image window to ensure it is the active window.
    2. In the OsiriX menu, click the **"WL/WW"** drop down menu and then click **"set WL/WW manually"**.
    3. When the drop down box appears in the active PET window, fill in the desired minimum intensity value in the **"From"** field and the desired maximum intensity value in the **"To"** field (*e.g.* to window the PET image from 0 to 20 SUV, type 0 into the "from" field and 20 into the "to" field).
    4. Alternatively, if it is desired to always load images with the same intensity values, in the top menu highlight **Osirix** - > **PET** - > then under **"Window Level & Width"** section, click the **Use fixed levels** bubble and insert the desired values in the **"From"** and **"To"** fields.

3. Once the desired lymph node is determined, manually draw an ROI around the edges of the lymph node.
    1. Highlight the PET/CT fusion image to ensure that it is the active window.
    2. As it is useful to use a multicolored color look-up table for this analysis, to change this setting: click on the **"CLUT"** dropdown box in the main OsiriX toolbar and select the desired lookup table setting (UCLA preferred).
    3. To draw a manual ROI around the lymph node, click the drop down menu on the right side of the **"Mouse Button Function"** in the main toolbar and select **"Closed Polygon"**. Click on the edge of the lymph node based on the PET windowing look up table to establish the first point of the ROI.
    4. Click on another point of the external edge of the lymph node and continue tracing until the lymph node is almost enclosed.
    5. To establish the final point of the ROI, double click to close in the ROI.
    6. Repeat this process on multiple slices to ensure determination of the maximum SUV within the lymph node.
    7. Record the desired SUV data in a separate spreadsheet.

## 6. Determination of FDG Muscle Background Uptake for Normalization of Values

NOTE: In order to maintain consistency over multiple imaging time points in regard to FDG uptake and the variation of metabolic activity in the animal at different times, all PET analysis should be normalized to muscle and presented as such. All quantitative PET data presented in this work is represented as a SUVCMR (Standard Uptake Value Cylinder Muscle Ratio).

1. Open PET and CT DICOM images from OsiriX database in the axial orientation (CT image will be fused with the PET image and there will be a separate PET image window).
2. Click on the Co-registered PET and CT image to ensure that it is the active window.
3. Scroll through the image until the slice containing the meeting point of the main bronchial tubes (carina) is reached.
4. Draw ROIs on back muscle to obtain background SUV values.
    1. Select the ROI dropdown tool on the right of the **"Mouse Button Option"** in the OsiriX main menu.
    2. Highlight **"Oval"** as the ROI tool.
    3. Draw ROIs of approximately the same size on the muscles located posterior and lateral to the spinal column.
    4. Click on the icon to the left of the Co-registered PET/CT scan and drag the icon to the PET window.

5. Select **"Copy ROIs"**. The ROIs should now be seen on the PET scan window.
6. On the main menu, select the **"Mode"** checkbox and make sure **"MIP – Max Intensity Projection"** is selected in the drop down menu immediately to the right.
7. Ensure that the **"Thick slab"** sliding scale is set to **10**. This indicates that 10 slices are combined on the PET image as a maximum intensity projection making a "cylinder" volume of interest (origin of cylinder muscle ratio).

5. Record the mean SUV values of the two ROIs in a spreadsheet.
6. Average the two values to obtain the background FDG muscle uptake value. This is the value used to obtain any ratio values between uptake at the target site and basal metabolic uptake.

## Representative Results

*Identification and Analysis of Individual Lesions*

Individual granulomas can be visualized for number, size, and FDG uptake qualitatively to understand the general scope of the infection process (**Figure 1**). Using these images, counting granulomas over time is a quantitative measure of disease spread. **Figure 2** depicts individual granuloma counts over time in a group of 10 animals. Of the 10 animals, three developed active disease and six developed latent infection. One animal showed no signs of active disease but was occasionally culture positive (in gastric aspirate and/or bronchoalveolar lavage samples) for *M. tuberculosis*, placing it within the spectrum of disease between active and latent and was thus removed from the analysis for this particular experiment. Of the three animals with active disease, one animal developed miliary disease by 12 weeks post-infection and was euthanized (this is identified in **Figure 2** as TNTC [Too Numerous To Count]). From 6 weeks after infection and thereafter, animals that would later develop active disease showed statistically higher numbers of granulomas than animals that would develop latent infection.

To better characterize and distinguish granulomas between active and latent animals, individual lesions on PET scans were analyzed to determine whether there was a difference in FDG uptake pattern between the two groups. In all of the active infection animals, there was an increase in FDG uptake in every granuloma from three to six weeks post infection (**Figure 3A**). Conversely, granulomas in animals that developed latent infection showed a variation in FDG uptake with some lesions increasing, decreasing, or showing the same uptake from three to six weeks (**Figure 3B**). These results are compared in groups showing the difference in change between latent and active animals at three weeks vs. six weeks (**Figure 3C**) and three weeks *vs.* 24 weeks (**Figure 3D**). In both cases, the granulomas of active animals showed a positive and significantly different change in SUV (within each individual animal (**Figure 3A and 3B**) and when compared by groups of animals (**Figure 3C and 3D**).

*Analyzing FDG Uptake in "Hot" Lymph Nodes*

As mediastinal lymph nodes are not readily visualized on CT scans unless greatly enlarged, PET images must be used to identify these diseased tissues. When analyzing lymph nodes, it is critical that the image is always scaled to the same maximum and minimum PET scale to maintain consistency throughout the process. When comparing the MLNs of animals that developed active or latent disease, Lin et al. showed through ROI analysis of MLNs that while FDG uptake in lymph nodes were similar between active and latent animals at 3 weeks, MLNs from active animals showed significantly higher uptake at 6 weeks[11]. Differences were seen to a greater degree at 8 and 12 weeks (**Figure 4**). Thus, PET/CT data can be utilized to assess significant differences in lymph nodes in addition to studying granulomas in infected animals.

*Total Lung FDG Avidity*

As an example of the power of evaluating total lung FDG avidity, Lin et al. showed that elevated lung inflammation in animals clinically classified as LTBI correlates with risk of reactivation[6]. In this study, LTBI cynomolgus macaques (infected with low-dose *M. tuberculosis*) were PET/CT imaged (6 months post-infection) prior to tumor necrosis factor (TNF) neutralization to assess the spectrum of lesions seen in clinically defined LTBI and determine risk of reactivation. Animals with higher total lung FDG avidity were more likely to reactivate (**Figure 5**). Over 90% of the animals with more than $10^3$ lung FDG avidity or with visible (by scan) at least one extra-pulmonary site of infection reactivated after TNF neutralization. Only one animal that did not reactivate exceeded this total lung FDG avidity threshold. Thus, PET/CT parameters can be a powerful tool to predicting clinical outcome though the specific parameters must be scientifically identified.

As an example to show utility in drug treatment scenarios, Coleman et al. conducted a study testing oxazolidinones in humans and cynomolgus macaques where total lung FDG avidity was measured pre-drug treatment, and one and two months post-treatment[10]. Fold changes were calculated to show drug response one month (**Figure 6A**) and two months post-treatment (**Figure 6B**). At both time points, control animals showed significantly higher FDG avidity in the entire lung space than drug-treated animals. In all of the drug-treated animals, total lung inflammation decreased over the two-month treatment regimen, while in most of the control animals, total lung inflammation increased over time or was unchanged.

 

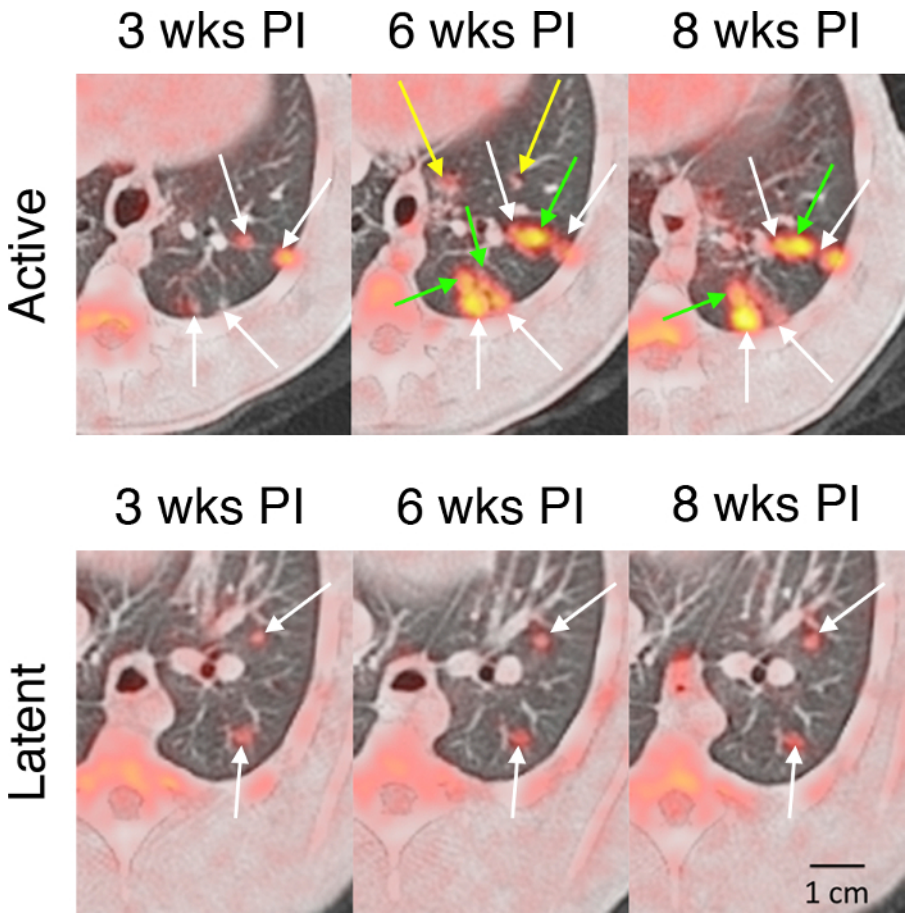


**Figure 1. Serial FDG PET/CT Images Showing a Disseminating and Stable Pattern of Granuloma Evolution During the Course of Early Infection.**
(Top row) Primary granulomas (white arrows) were first established at 3 weeks post-infection, while new granulomas developed adjacent to existing lesions (green arrows) or in new sites (yellow arrows). Animals that would later develop active TB developed more lesions during the course of infection. (Bottom row) Primary granulomas (white arrows) of latent animals usually remained stable, with few new granulomas developing through the course of infection. wks PI, weeks post-infection. Figure taken from Coleman *et al.*[11] Please click here to view a larger version of this figure.

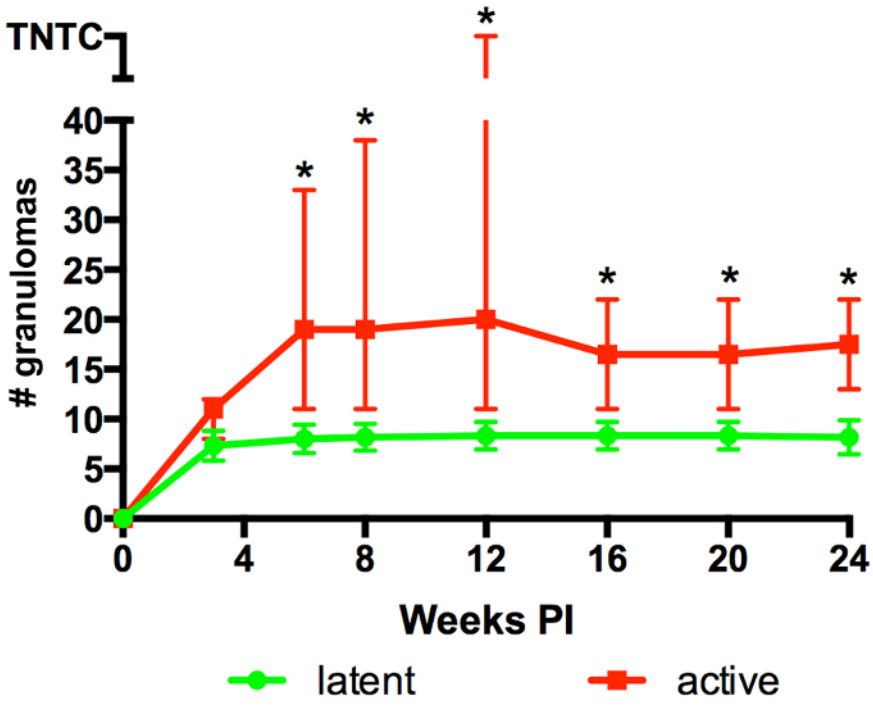


**Figure 2. Representative Data of Depicting the Median and Range of Granuloma Counting from CT Scans Comparing Animals with Active Infection (Red Symbols) to Latent Infection (Green Symbols).**
Active infection animals had more granulomas than latently infected animals as early as six weeks post-infection. P < 0.05 (*) by Mann-Whitney test. Weeks PI, weeks post-infection. TNTC, too numerous to count. Figure adapted from Coleman *et al.*[11] Please click here to view a larger version of this figure.

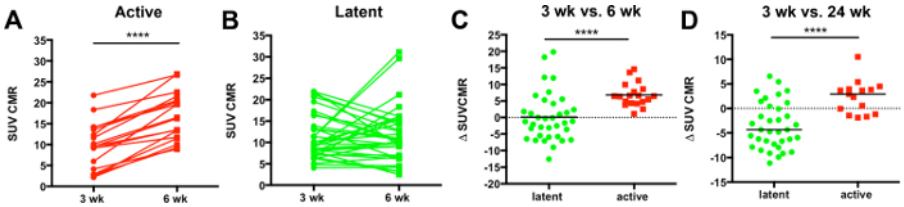


**Figure 3. Utilization of ROI Analysis on PET Images to Show that Metabolic Activity of Lung Granulomas Differs Between Active and Latently Infected Animals During Early Infection.**
Individual granulomas in active animals [A] have a significant increase in metabolic activity (measured as standard uptake value normalized to muscle uptake [SUVCMR]) between 3 and 6 weeks after infection while latently infected animals [B] do not. The change in metabolic activity in lesions between latent and active animals as groups were compared at 3 vs. 6 weeks [C] and 3 *vs.* 24 weeks [D] showing that actively infected animals (red squares) have a significantly larger change in uptake than latent animals (green circles) at both time points. Solid black lines represent the median. The Wilcoxon rank-sum test was used to analyze data in panels A and B. For panels C and D, values were analyzed by the Mann-Whitney test. P < 0.0001 (****) for all panels. Figure adapted from Coleman *et al.*[11] Please click here to view a larger version of this figure.

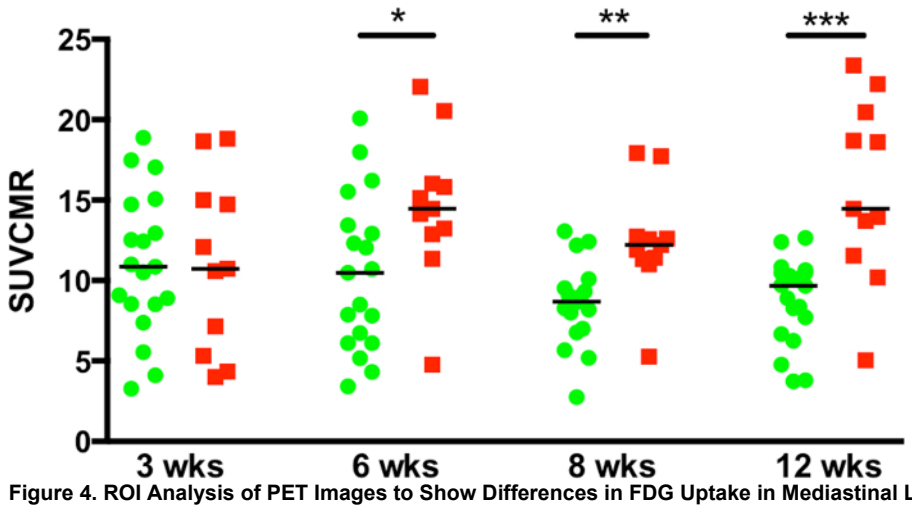


**Figure 4. ROI Analysis of PET Images to Show Differences in FDG Uptake in Mediastinal Lymph Nodes Between Animals with Active Disease (Red Squares) and Latent Disease (Green Circles).**
Uptake was higher in actively infected animals at 6, 8, and 12 weeks post infection. Each dot represents an individual lymph node. Solid black lines represent the median. $P < 0.05$ (*), $P < 0.01$ (**), and $P < 0.001$ (***) by Mann-Whitney test. Figure adapted from Coleman *et al.*[11] Please click here to view a larger version of this figure.

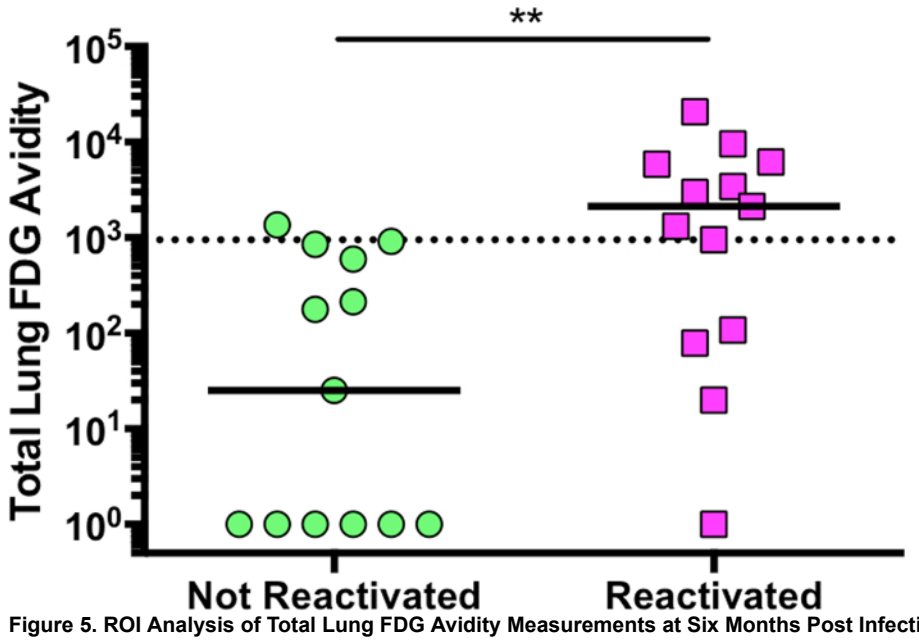


**Figure 5. ROI Analysis of Total Lung FDG Avidity Measurements at Six Months Post Infection Highlighting Differences in FDG Uptake in Animals Which Reactivate from Latent Infection (Pink Squares) in Comparison to Animals Which Remain Latent (Green Circles).**
Three of the four "reactivated" animals that lie below the dotted line had extra-pulmonary disease prior to TNF (tumor necrosis factor) neutralization. Each dot represents one animal. Dotted line represents threshold value for likely reactivation risk. Solid black lines represent the median. $P < 0.01$ (**) from Mann-Whitney Test. Data adapted from Lin *et al.*[6] Please click here to view a larger version of this figure.

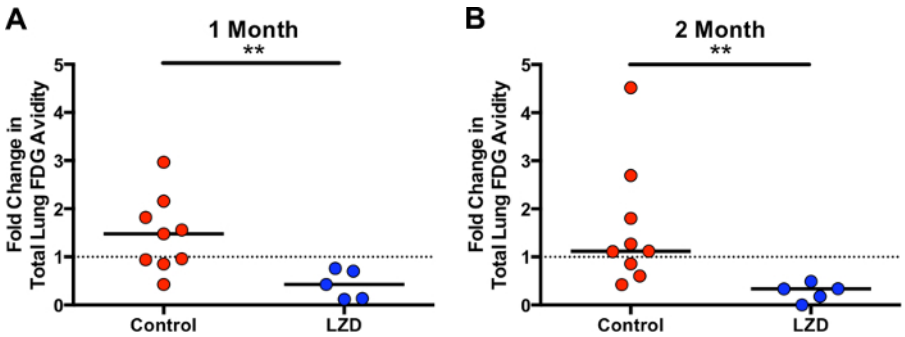


**Figure 6. Representative Total Lung FDG Avidity ROI Measurements Highlighting Overall Change in Inflammation Measured in Lungs Comparing Untreated (Red Circles) and Linezolid Treated (Blue Circles) Monkeys.**
FDG avidity was measured before linezolid treatment (30 mg/kg daily) and the fold change in total FDG uptake was measured at 1 month [A] and 2 months [B] post treatment. Each monkey is represented by an individual circle. Solid black lines represent the median. P < 0.01 (**) per Mann-Whitney Test. Please click here to view a larger version of this figure.

## Discussion

Data acquired from PET/CT can be used as surrogate measurements for many aspects of *M. tuberculosis* infection that would be unobservable without such technology. PET/CT is much more sensitive than X-ray technology, which is often used in macaques studies. PET/CT provides structural, spatial and functional information. The analyses described above have many practical applications such as monitoring disease progression, assessing effectiveness of drug treatment, and providing risk factors for reactivation[6,10,11,13].

Tracking the spread of granulomas and FDG uptake of individual lesions can be compared between control and experimental groups to not only provide specific location of the infection, but also follow dissemination of disease[25]. For example, in work from Coleman et al. describing early infection in cynomolgus macaques, following the infection progression can determine whether the infection within an animal is going to remain active and worsen or be contained by the immune system (*i.e.* LTBI)[11]. This is just one example of the power that PET/CT imaging has in studying the progression of disease with respect to granulomas. The same method can be used to study a wide variety of experimental parameters over time. For example, enumeration of granulomas that establish by 4 weeks post-infection can provide a powerful outcome measure for a vaccine, since the best vaccines would prevent or limit granuloma establishment following challenge. Another outcome measure for vaccines could be in limiting dissemination. These quantifiable outcome measures provide important data without the need to perform early necropsies on the animals. A limitation of assessing individual granulomas is the sensitivity of the CT scanner; visualizing granulomas <1 mm in size is often not possible.

Evaluation of mediastinal lymph nodes (MLNs) is important when studying *M. tuberculosis* infection as well. MLNs are important for T-cell priming and trafficking of immune cells during infection. However, in nearly all macaques, at least one, and sometimes several MLNs can become infected. Thus, MLNs are an additional site of bacterial persistence during active TB and LTBI, and can serve as a reservoir for bacteria, possibly contributing to reactivation[26,27]. In cases of severe MLN involvement, airways can be compressed. Large necrotic MLNs can erode into the airways, leading to dissemination of the infection. Analyzing PET/CT data on lymph nodes is more complex than granulomas because the structural components of the nodes are not readily visible on CT scans. Additionally, only the lymph nodes that are metabolically active can be analyzed due to FDG uptake. Because of this, when analyzing hot lymph nodes, it is important to ensure that the PET image is scaled to the same maximum and minimum intensity scale for each image analysis to ensure consistency. Since they can be large structures, the necrotic center can be negative for FDG avidity, and thus FDG avidity can appear to be reduced over time, even when disease is increasing in the MLNs.

Total lung FDG avidity represents the total inflammation within the lungs. The amount of lung inflammation is an indication of disease severity and is correlated with bacterial burden[6,10,28] therefore this quantitative and objective assessment has numerous applications. To measure total FDG avidity, all voxels within a PET image that show an SUV of greater than 2.3 are combined in a single volume-of-interest (VOI) and the total SUV value of the entire VOI is the final avidity value. This value was selected from literature that compared SUV values of FDG uptake in lung tumors to various infectious pathologies in humans[24]. It is important to note that this total FDG avidity value is limited only to disease in the lung space and all FDG uptake non-disease related or located in close proximity to the lungs must not be considered. In addition, total lung FDG avidity does not include MLNs. While the avidity of individual granulomas and lymph nodes allows us to see the variability of TB outcomes within the host, FDG avidity of the total lung is integral to evaluating the host as a whole. These methods also function as analytical tools to measure drug response to TB disease. Previous work has shown that TB drug treatment can reduce the size and FDG avidity of individual granulomas over time[12] and these changes were associated with reduced bacterial burden. Changes in inflammation over the full course of drug regimens can also be used to assess drug efficacy or failure.

Due to the highly detailed nature of these procedures, a fair amount of troubleshooting may be necessary in order to obtain the most consistent data during studies. It is the goal of this paper to outline the procedures to enable individuals throughout the world to use these techniques while keeping in mind that precise attention to detail is essential. Persons evaluating images should be very familiar with anatomy and physiology in order to recognize abnormality within particular scans. Image readers need to recognize non-normal probe uptake throughout the body because TB can spread beyond the thoracic cavity. Additionally, PET and CT registration in imaging is not a perfect process and occasional deviations on image registration can occur; recognizing this can be vitally important when evaluating very small disease features (*i.e.* 1 - 2 mm granulomas). A pre-infection scan can be particularly useful as a comparator to identify normal lung (and other organ) structures and PET patterns and recognize those that are new or changed post-infection. Another important component to this analysis is background measurement. All PET data are normalized to muscle uptake as a physiological baseline because FDG uptake is based on metabolism. A combination of rhomboid and serratus muscles in the back are used for background measurements because of proximity to the thoracic cavity and relative consistency in FDG uptake in fasted animals. In the case of *M. tuberculosis*-infected macaques, this is preferable to using another organ, such as the liver, for background

measurements as *M. tuberculosis* can infect the liver and liver metabolism can be affected when treating animals with various anti-TB drugs. Taking the above factors into account as well as ensuring that all image regions-of-interest are saved at the end of analysis should yield highly reproducible results.

In summary, PET/CT offers a unique and powerful method for investigating *M. tuberculosis* infection in non-human primates, providing quantitative outcome measures that relate to initial infection, dissemination, and bacterial burden. This allows for tracking the variable outcomes of infection across individual animals without the need for necropsies at various time points, thus saving resources and reducing animal use. This technology is directly translatable to humans, as PET/CT has been used in several studies to assess drug treatment in TB, as well as LTBI in HIV- and HIV+ subjects[10,29,30,31]. Finally, this technology and quantitative tool set for analyzing PET/CT data are likely to be useful in the future for vaccine efficacy studies and can likely be used as a template for analysis of other infectious diseases in animal models and human subjects.

## Disclosures

The authors have nothing to disclose.

## Acknowledgements

The authors wish to acknowledge Mark Rodgers for outlining the infection procedures and L. Eoin Carney and Brian Lopresti for guidance in establishing these imaging procedures. Funding for this work has been provided by The Bill and Melinda Gates Foundation (J.L.F., P.L.L.), National Institutes of Health, National Institutes of Allergy and Infectious Diseases R01 AI111871 (P.L.L.), National Heart Lung and Blood Institute R01 HL106804 (J.L.F.), R01 HL110811.

## References

1. *Global Tuberculosis Report 2016.* <http://www.who.int/tb/publications/global_report/en/> (2017).
2. Barry, C. E., 3rd *et al.* The spectrum of latent tuberculosis: rethinking the biology and intervention strategies. *Nat Rev Microbiol.* **7** (12), 845-855 (2009).
3. Lin, P. L., & Flynn, J. L. Understanding latent tuberculosis: a moving target. *J Immunol.* **185** (1), 15-22 (2010).
4. Pawlowski, A., Jansson, M., Skold, M., Rottenberg, M. E., & Kallenius, G. Tuberculosis and HIV co-infection. *PLoS Pathog.* **8** (2), e1002464 (2012).
5. Keane, J. TNF-blocking agents and tuberculosis: new drugs illuminate an old topic. *Rheumatology (Oxford).* **44** (6), 714-720 (2005).
6. Lin, P. L. *et al.* PET CT Identifies Reactivation Risk in Cynomolgus Macaques with Latent *M. tuberculosis. PLoS Pathog.* **12** (7), e1005739 (2016).
7. Flynn, J. L., Klein, E. *A color atlas of comparative pulmonary tuberculosis histopathology.* (ed Dick T. Leong V.D.J.) 83-106 CRC (2011).
8. Signore, A., Mather, S. J., Piaggio, G., Malviya, G., & Dierckx, R. A. Molecular imaging of inflammation/infection: nuclear medicine and optical imaging agents and methods. *Chem Rev.* **110** (5), 3112-3145 (2010).
9. James, M. L., & Gambhir, S. S. A molecular imaging primer: modalities, imaging agents, and applications. *Physiol Rev.* **92** (2), 897-965 (2012).
10. Coleman, M. T. *et al.* PET/CT imaging reveals a therapeutic response to oxazolidinones in macaques and humans with tuberculosis. *Sci Transl Med.* **6** (265), 265ra167 (2014).
11. Coleman, M. T. *et al.* Early Changes by (18)Fluorodeoxyglucose positron emission tomography coregistered with computed tomography predict outcome after Mycobacterium tuberculosis infection in cynomolgus macaques. *Infect Immun.* **82** (6), 2400-2404 (2014).
12. Lin, P. L. *et al.* Radiologic Responses in Cynomolgus Macaques for Assessing Tuberculosis Chemotherapy Regimens. *Antimicrob Agents Chemother.* **57** (9), 4237-4244 (2013).
13. Diedrich, C. R. *et al.* Reactivation of latent tuberculosis in cynomolgus macaques infected with SIV is associated with early peripheral T cell depletion and not virus load. *PLoS One.* **5** (3), e9611 (2010).
14. Lin, P. L. *et al.* The multistage vaccine H56 boosts the effects of BCG to protect cynomolgus macaques against active tuberculosis and reactivation of latent Mycobacterium tuberculosis infection. *J Clin Invest.* **122** (1), 303-314 (2012).
15. Lin, P. L. *et al.* CD4 T cell depletion exacerbates acute Mycobacterium tuberculosis while reactivation of latent infection is dependent on severity of tissue depletion in cynomolgus macaques. *AIDS Res Hum Retroviruses.* **28** (12), 1693-1702 (2012).
16. Mattila, J. T., Diedrich, C. R., Lin, P. L., Phuah, J., & Flynn, J. L. Simian immunodeficiency virus-induced changes in T cell cytokine responses in cynomolgus macaques with latent Mycobacterium tuberculosis infection are associated with timing of reactivation. *J Immunol.* **186** (6), 3527-3537 (2011).
17. Scanga, C. A., Flynn, J.A. in *Tuberculosis.* (ed S.H.E. Kaufmann, Rubin, E.J., Zumla, A.) 243-258 Cold Spring Harbor Laboratory Press (2015).
18. Kita, Y. *et al.* Development of therapeutic and prophylactic vaccine against Tuberculosis using monkey and transgenic mice models. *Hum Vaccin.* **7 Suppl** 108-114 (2011).
19. Langermans, J. A. *et al.* Divergent effect of bacillus Calmette-Guerin (BCG) vaccination on Mycobacterium tuberculosis infection in highly related macaque species: implications for primate models in tuberculosis vaccine research. *Proc Natl Acad Sci U S A.* **98** (20), 11497-11502 (2001).
20. Okada, M. *et al.* Novel prophylactic and therapeutic vaccine against tuberculosis. *Vaccine.* **27** (25-26), 3267-3270 (2009).
21. Reed, S. G. *et al.* Defined tuberculosis vaccine, Mtb72F/AS02A, evidence of protection in cynomolgus monkeys. *Proc Natl Acad Sci U S A.* **106** (7), 2301-2306 (2009).
22. Capuano, S. V., 3rd *et al.* Experimental Mycobacterium tuberculosis infection of cynomolgus macaques closely resembles the various manifestations of human M. tuberculosis infection. *Infect Immun.* **71** (10), 5831-5844 (2003).
23. Srinivas, S. M. *et al.* A recovery coefficient method for partial volume correction of PET images. *Ann Nucl Med.* **23** (4), 341-348 (2009).

 

24. Kumar, R. *et al.* Role of modern imaging techniques for diagnosis of infection in the era of 18F-fluorodeoxyglucose positron emission tomography. *Clin Microbiol Rev.* **21** (1), 209-224 (2008).
25. Martin, C. J. *et al.* Digitally Barcoding Mycobacterium tuberculosis Reveals In Vivo Infection Dynamics in the Macaque Model of Tuberculosis. *MBio.* **8** (3) (2017).
26. Lin, P. L. *et al.* Metronidazole prevents reactivation of latent Mycobacterium tuberculosis infection in macaques. *Proc Natl Acad Sci U S A.* **109** (35), 14188-14193 (2012).
27. Lin, P. L. *et al.* Tumor necrosis factor neutralization results in disseminated disease in acute and latent Mycobacterium tuberculosis infection with normal granuloma structure in a cynomolgus macaque model. *Arthritis Rheum.* **62** (2), 340-350 (2010).
28. Phuah, J. *et al.* Effects of B Cell Depletion on Early Mycobacterium tuberculosis Infection in Cynomolgus Macaques. *Infect Immun.* **84** (5), 1301-1311 (2016).
29. Martinez, V., Castilla-Lievre, M.A., Guillet-Caruba, C., Grenier, G., Fior, R., Desarnaud, S., Doucet-Populaire, F., and Boue, F. (18)F-FDG PET/CT in tuberculosis: an early non-invasive marker of therapeutic response. *Int J Tuberc Lung Dis.* **16** (9), 1180-1185 (2012).
30. Malherbe, S. T. *et al.* Persisting positron emission tomography lesion activity and Mycobacterium tuberculosis mRNA after tuberculosis cure. *Nat Med.* **22** (10), 1094-1100 (2016).
31. Chen, R. Y. *et al.* PET/CT imaging correlates with treatment outcome in patients with multidrug-resistant tuberculosis. *Sci Transl Med.* **6** (265), 265ra166 (2014).


 